Power Electronics and Drives
Volume 10(45), 2025 DOI: 10.2478/pead-2025-0019

Power Electronics and Drives

Experimental analysis for star and open-end stator winding structures of IM

Research paper

Abdelmonoem Nayli[1,*], Sami Guizani[2,3], Faouzi Ben Ammar[3]

[1]University of Gafsa, IPEIG, Gafsa, Tunisia
[2]University of EL Manar, IPEIEM, Tunisia, Tunisia
[3]University of Carthage, MMA Laboratory, INSAT, Tunisia, Tunisia

Received: 05 July, 2025; Received in the revised form: 07 August, 2025; Accepted: 23 August, 2025

Abstract: This article focuses on the scalar control of four induction machine structures: the conventional induction machine, the double-star machine, the open-ended stator winding machine and the dual open-end stator winding machine. To compare these different structures under the same conditions, we used a single induction machine prototype to design these four machine structures. In addition, we also developed a single scalar control algorithm to control these four machines, which is implemented in a field-programmable gate array board FPGA. The experimental results showed the efficiency of the operation of this prototype as well as that of the algorithm developed for the four machines. The experimental results also presented the significant advantage of open-end stator winding structures over star winding structures. The increase in three-phase windings allows for better power segmentation, which is better when the three-phase stator windings are open-ended.

Keywords: *induction machine • double star machine • open-end stator winding machine • dual three-phase open-end stator windings machine • power segmentation*

1. Introduction

Induction machines that are associated with converters are constantly found in applications in the industry (Jahns, 1980; Nelson and Krause, 1974). The feeding of these machines for the great powers became possible thanks to the evolution of semiconductor components, but with relatively low switching frequencies.

To remedy this problem, research laboratories have been continuously trying to find solutions at the level of the converter or machine by trying to segment the power.

This power segmentation is obtained by use of the following:

- A number of phases superior than three, where each phase is fed by its own single-phase inverter (Figure 1a) or by a multi-leg inverter having a number of arms equal to the number of phases (Figure 1b); this is the multi-phase induction machine (Abbas et al., 1984; Singh et al., 2003).
- A multiple number of three phases connected in star which is the multi-star machine. One of such machines is the double star induction machine 'DSIM', as shown in Figure 2. The first machine of synchronous type was designed essentially for current power supplies with a shift of 30° between the two stars to improve the quality of the torque (Alger, 1928). It was the subject of several studies for voltage supply and for different shifts between the two three-phase stator windings 0°, 30° and 60°, although for the latter shift it was shown that with a good choice of control, an equivalent machine is obtained than with a shift 0°. The double star machines also have the possibility to operate in active or passive redundancy and allow consequently to improve the reliability of the drive systems (Guizani and Ben Ammar, 2008; Jacek, 2018; Xueqing et al., 2018).

* Email: abdelmonoem.nayli@gmail.com

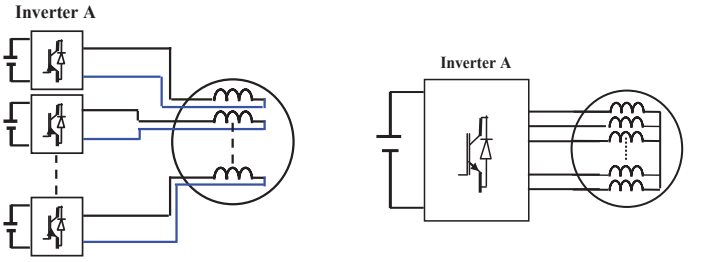

(a): Multiphase IM supplied by H-Bridges inverters

(b): Multiphase IM supplied by multi- leg inverters

Figure 1. Multi-phase induction machine.

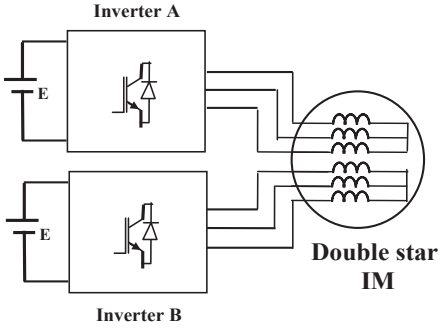

Figure 2. Double star induction machine supplied by two voltage source inverters.

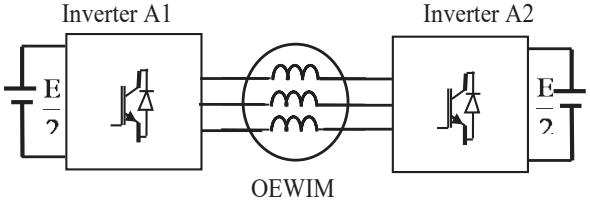

Figure 3. Open-end stator winding IM supplied by two voltage source inverters.

Other machine structures are the open-end stator windings induction machine structures which offer power segmentation and the possibility to operate in degraded mode. These machines include as follows:

- Three-phase open-end stator winding induction machine 'OEWIM' as shown in Figure 3 (Chatterjee and Kastha, 2024; Kalaiselvi and Srinivas, 2015; Monteiro et al., 2022; Sandulescu et al., 2013; Somasekhar et al., 2004; Yu et al., 2025; Zerdani et al., 2023).
- The induction machine having a number of phases superior to three open-end stator windings. Then, it is the multiphase open-end stator windings machine (Bodo et al., 2013; Jiang et al., 2023; Levi et al., 2012). Each phase can be fed by two single-phase inverters (Figure 4a), or by two multi-leg inverters (Figure 4b).
- The induction machine having two open three-phase stator windings. Each winding is powered by two inverters, as shown in Figure 5. Although this structure is very recent in research, it combines the advantages of the double-star machine and those of the open stator winding machine. It offers good dynamic performance (Guizani and Ben Ammar, 2018; Nayli et al., 2017). It allows for better power segmentation and increases the degrees of freedom of the drive system in degraded mode. Indeed, a failure in one of the inverters does not stop the system from operating (Guizani and Ben Ammar, 2013). Furthermore, it offers the possibility of operating with passive or active redundancy (Guizani and Ben Ammar, 2015).

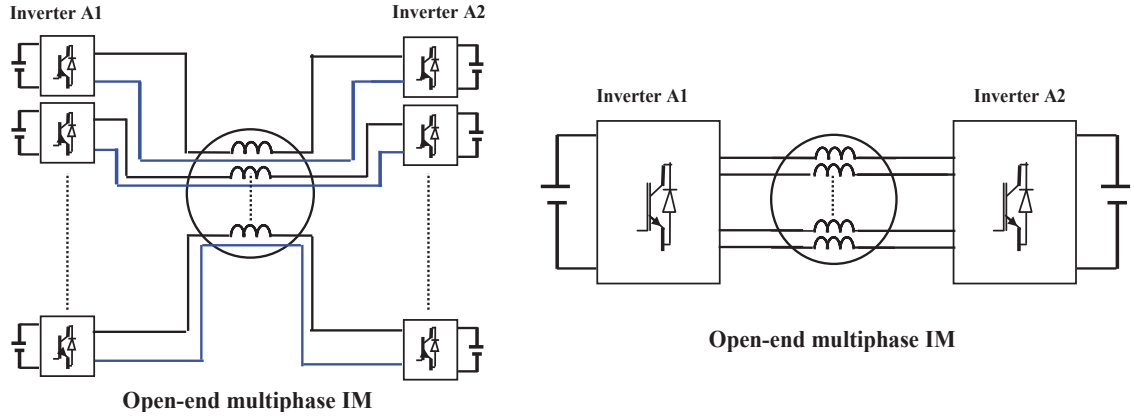

(a) open-end multiphase IM supplied by H-bridges inverter

(b) open-end multiphase IM supplied by two multi-leg inverter

Figure 4. Open-end multiphase IM.

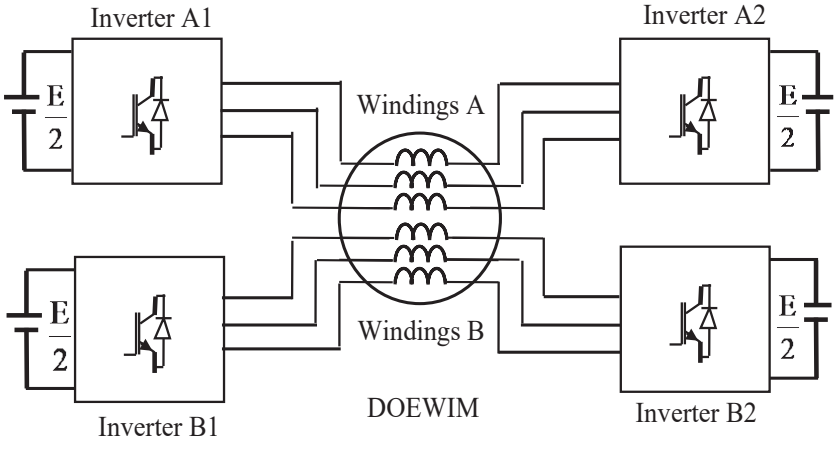

Figure 5. Dual open-end windings induction machine.

This paper deals with induction machines with star windings and three-phase open-end stator windings.

The prototype of an induction machine with a power of 1.5 kW with different stator winding structures is realised, including the conventional induction machine, double star induction machine, open-end winding induction machine and dual open-end winding induction machine. Each machine is fed by voltage source inverters based on V/f law when the control scalar (V/f) is implemented on FPGA board for control inverter. Then, the obtained experimental results of voltages and stator current for different machine structures are presented with interpretation of different results that present the advantages of induction machines with open-end stator winding.

2. Digitisation of the Command for Different Machine Structures

To show the scalar control, it is essential to vary the speed of the machine such that the ratio of the voltage and stator frequency is always constant.

To obtain this control in a transitional regime, generation of the three voltages references must be variable in amplitude and frequency during the acceleration phase.

To view the command signals of the inverters, the triangular signals are compared with three reference signals. Then the dead time is created in order to avoid any short circuit between the different switches. Figure 6 represents the diagram of the scalar control for the different blocks necessary to obtain the control signals for each inverter to supply the different machines.

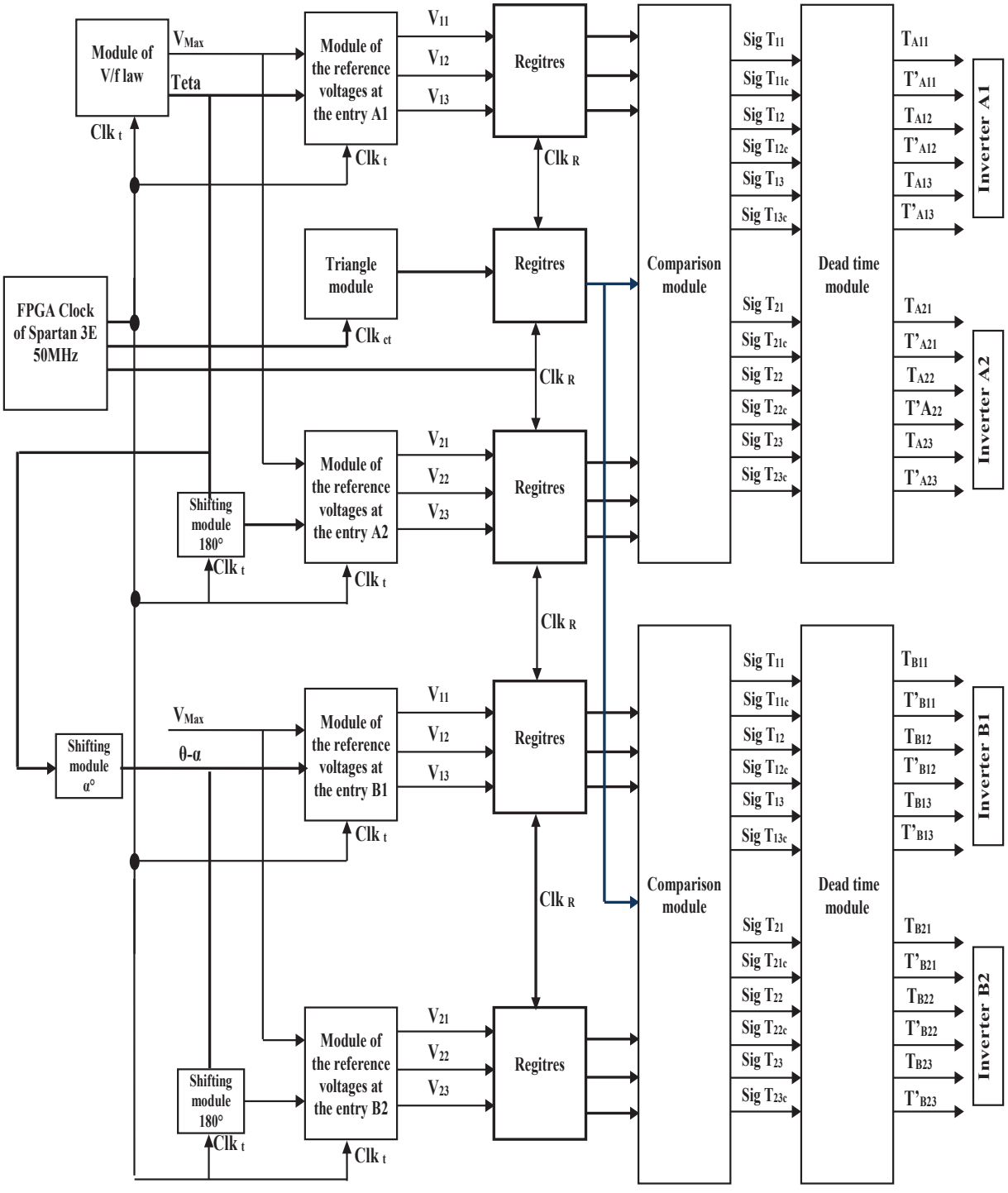

Figure 6. Diagram of the scalar control for the four machine structures.

The single scalar control algorithm is validated in MATLAB Simulink environment using a Xilinx System Generator, as represented in Figure 7. This control is used for implementation in an evaluation board Nexys 2 based on FPGA of the family SPARTAN 3E.

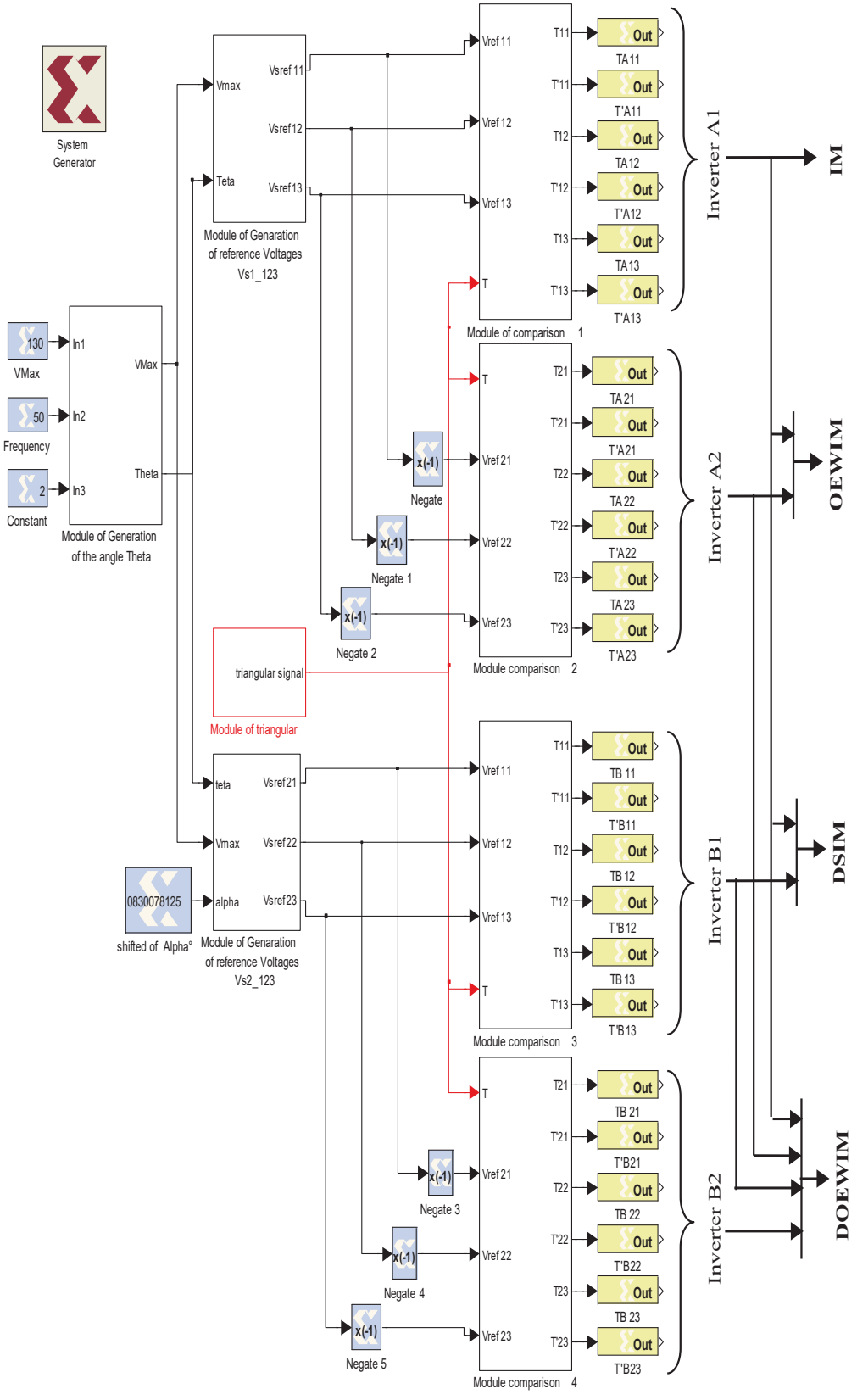

Figure 7. Scalar control using the Xilinx System Generator for the command of the four machines.

The operating procedure for the different machines is the same: it consists of a start cycle between $t = 0$ s and $t = 0.6$ s. We used the ramp for the reference signal, as shown in Figure 8.

The experimental results of the different command signals with the dead times 3μs at the output of the FPGA for the same carrier frequency 3,258 Hz for controlled different induction machine structures are indicated in Figure 9. Figure 9a shows the command signal T_{A11} of arm 1 of inverter A1 (the same as inverter B1) and the complement T'_{A11} obtained and dead time equal to 3 μs as shown in Figure 9b.

The obtained experimental results of the command signals of switches T_{A21} and complement T'_{A21} for inverter A2 (the same as inverter B2) is shown in Figure 10.

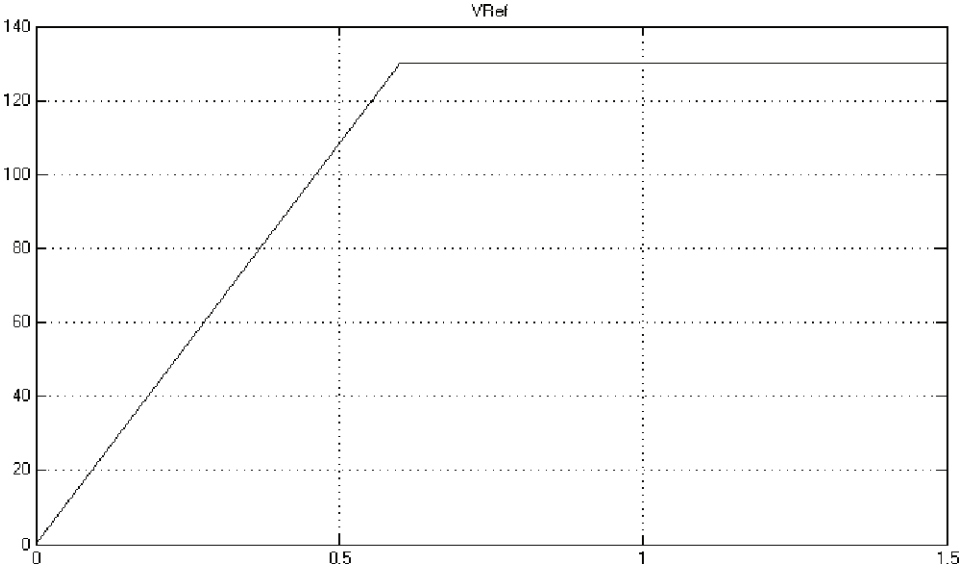

Figure 8. Reference signal for the speed ramp.

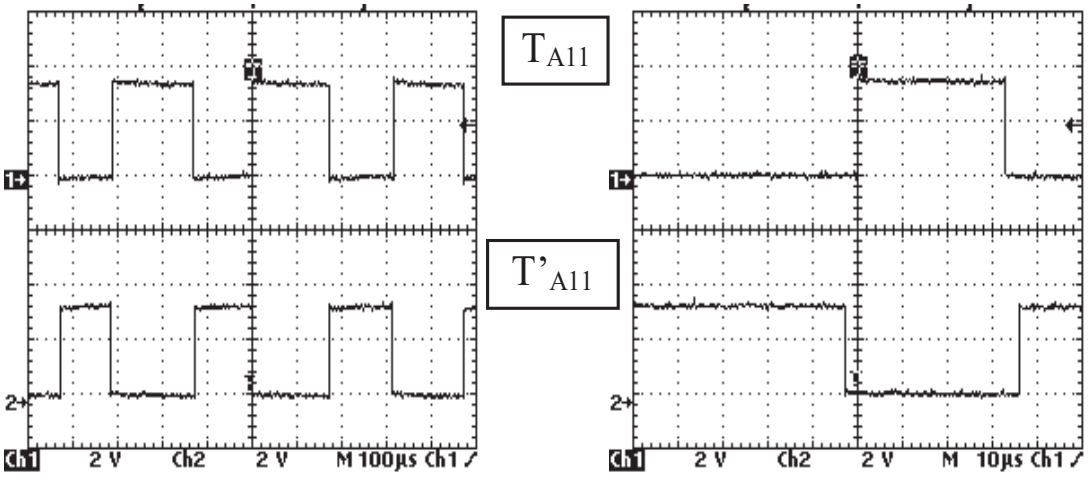

(a) switch T_{A11} and T'_{A11} (b) Dead-times (3μs)

Figure 9. Command signals for inverter A1 with dead-times.

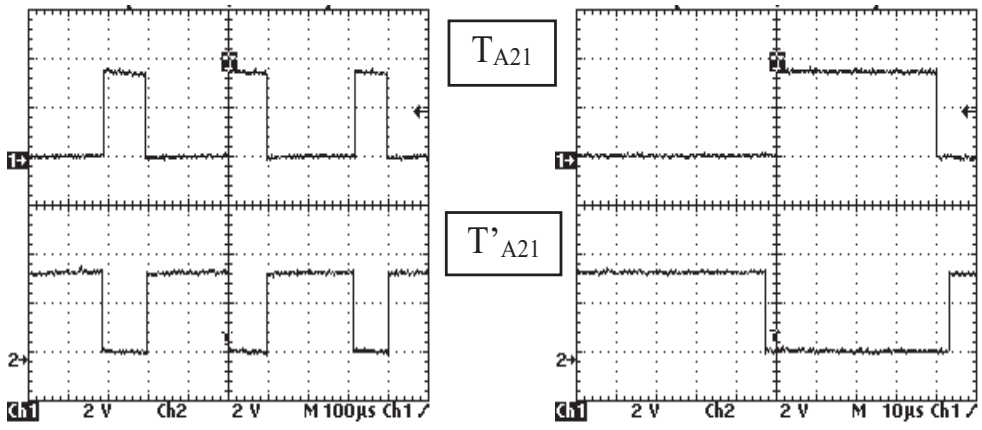

(a) Switch T_{A21} and T'_{A21} (b) Dead-times (3µs)

Figure 10. Command signals for inverter A2 with dead-times.

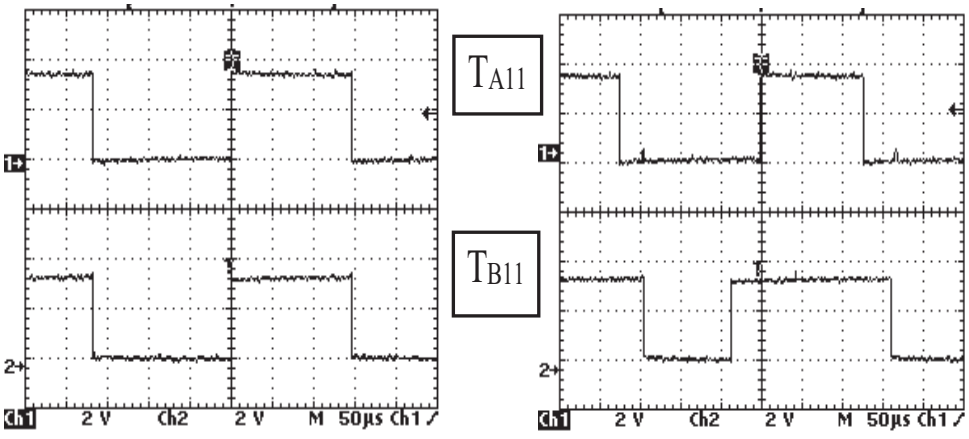

(a) DSIM - DOEWIM (0°) (b) DSIM - DOEWIM (30°)

Figure 11. Command signals for switches T_{A11} and T_{B11}.

Figure 11a shows the command signals of switches T_{A11} and T_{B11} for inverters A1 and B1 to supply the 'DSIM' and 'DOEWIM' by 0°. Figure 11b shows the command signals of the inverters (A1, B1) for 'DSIM' and 'DOEWIM' shifted by 30°.

3. Experimental Results for Different Machine Structures

To compare the performances between the four induction machine structures, only one prototype of a power induction machine $P = 1.5$ kW has been carried out; this prototype allows to have the four stator winding structures, as shown in Figure 12. The single algorithm scalar control controlled the inverters of type Semikron for supply to the different machine structures, whose controller is embedded into the Xilinx Spartan-3E FPGA board.

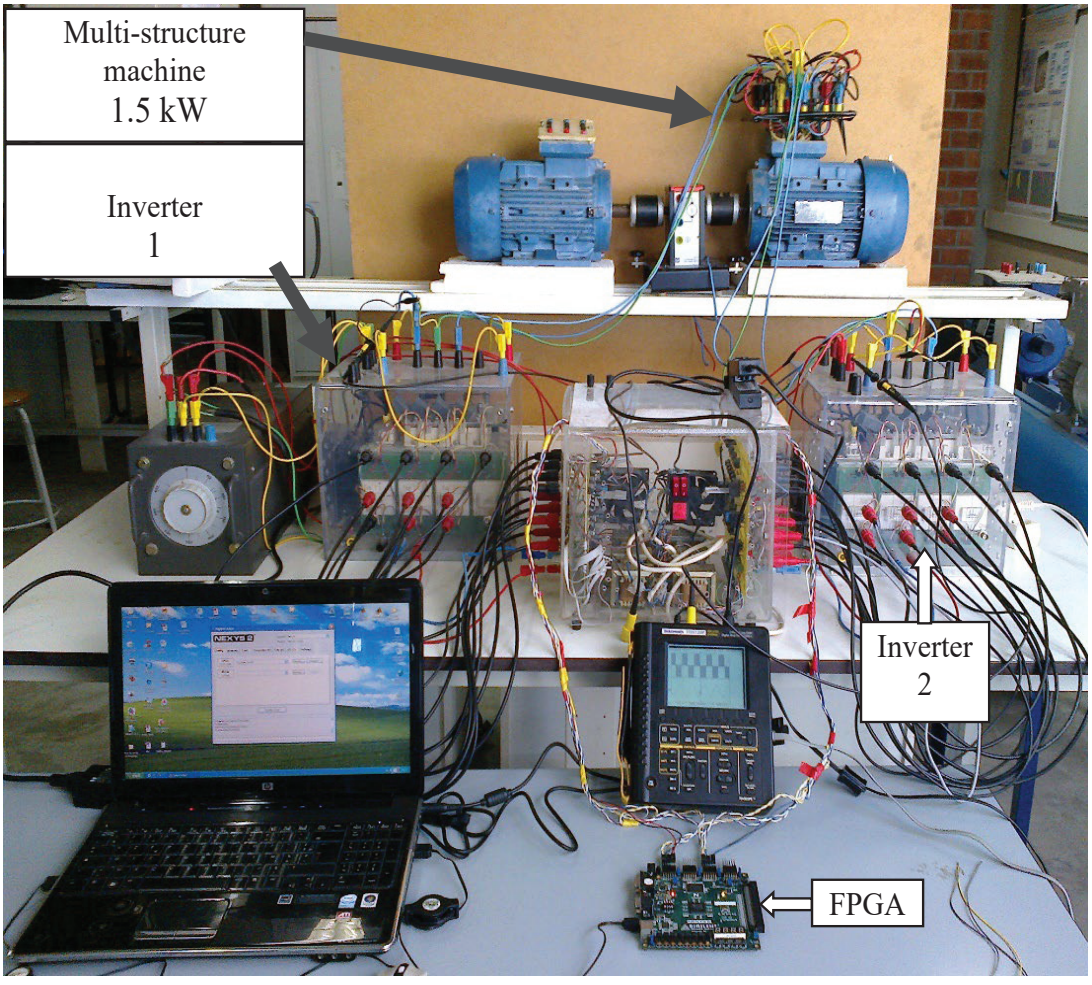

Figure 12. Experimental prototype for different stator winding structures of induction machine.

3.1. Experimental results for conventional induction machine

The machine is fed by a three-phase 2-level inverter with DC-link (E), whose inverter is dimensioned to a power P of the machine, as shown in Figure 13.

Figure 14 shows the evolution of voltage between phase of inverter A and stator current of phase in the starting time during 0.5 s of the induction machine.

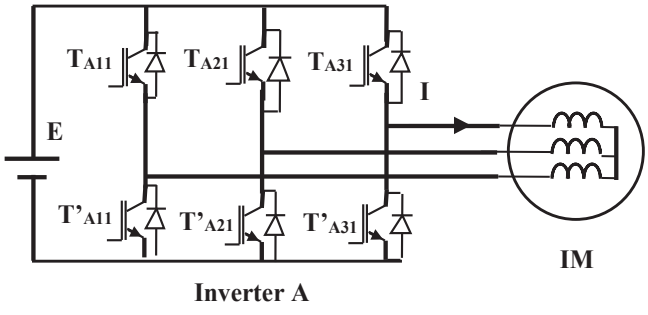

Figure 13. Induction machine supplied by voltage source inverter.

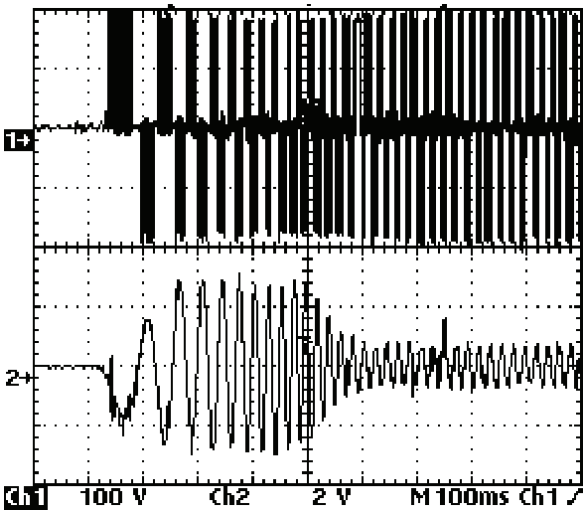

Figure 14. Evolution of voltage and stator current in starting of conventionnel IM.

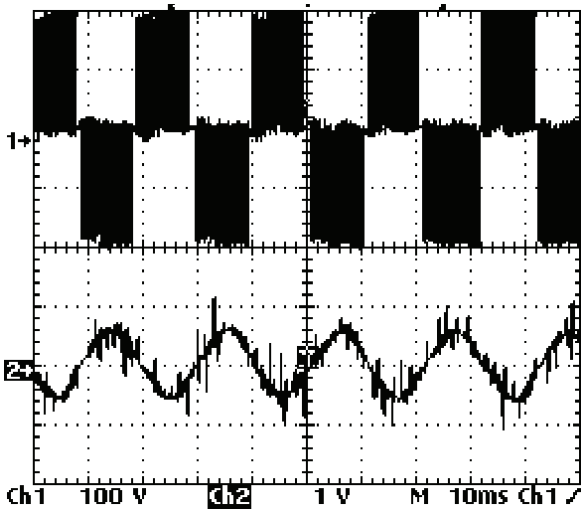

Figure 15. Enlarging effect of voltage and stator current in permanent mode of the conventional IM.

Thereafter, the operation is in permanent mode. Figure 15 shows an enlarging effect of voltage between phases and stator current during the steady-state operation.

3.2. Experimental results for double star induction machine

The double star asynchronous machine is fed by voltage source inverter based on V/f law to each star with DC-link (E). This structure is represented in Figure 16. Each inverter is dimensioned to a half-power of the machine.

Figure 17 shows the obtained experimental results of the starting time during 0.5 s and of the operation in permanent mode when the two three-phase stator windings is shifted by 0°. The two stator currents are shown in Figure 17a and the voltage between phases and stator current of star A is shown in Figure 17b. The enlarging effect of the operation in permanent mode showing the voltage between phases and stator current for the star A is shown in Figure 17c and the voltage between phases and stator current for the star B is shown in Figure 17d. These results present the reduction of the current source to give half-power of each inverter compared with the classic induction machine.

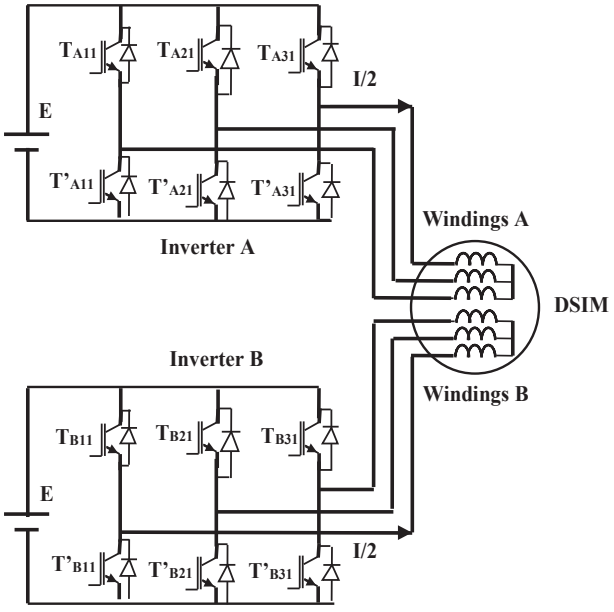

Figure 16. DSIM supplied by two voltage source inverters.

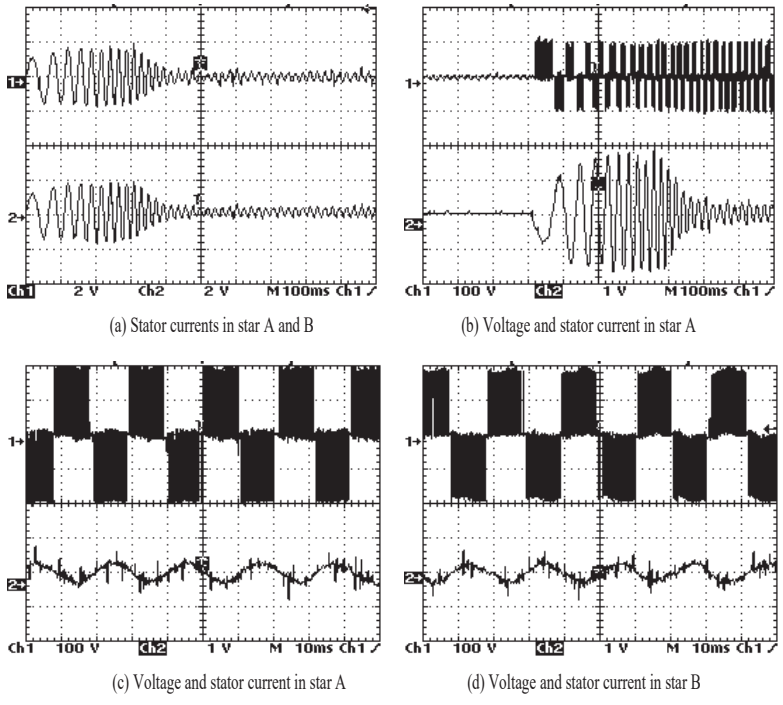

(a) Stator currents in star A and B

(b) Voltage and stator current in star A

(c) Voltage and stator current in star A

(d) Voltage and stator current in star B

Figure 17. Experimental results of the DSIM shifted by 0°.

In addition, the results of double star induction machine shifted by 30° in permanent mode such as the voltage of each inverter (A and B) and stator current of each star are as shown in Figure 18. These results present the improvement in the quality stator compared with the double star induction machine shifted by 0° and the classic induction machine.

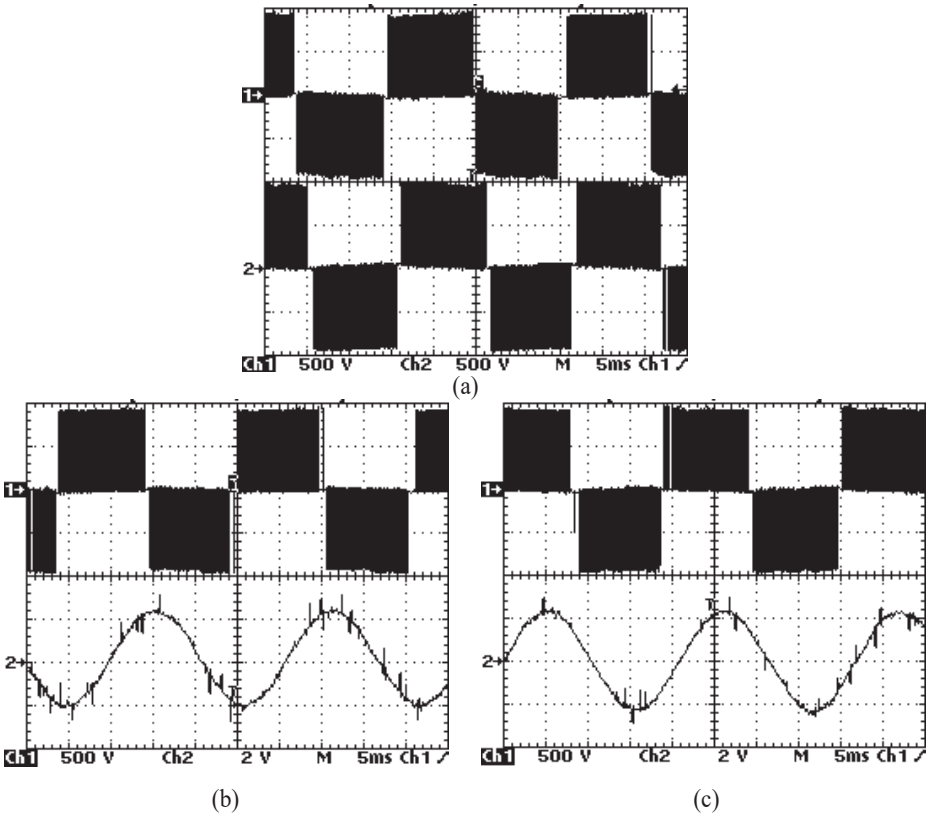

Figure 18. Experimental results of the double star winding IM shifted by 30°: (a) Voltage of inverters A and B; (b) Voltage of inverters A and stator current in star A and voltage of inverters B and stator current in star B.

3.3. Experimental results for open-end stator winding induction machine

The structure of the feeding open-end stator winding induction machine supplied by two voltage source inverters with half DC-link (E/2), as shown in Figure 19. Each inverter is dimensioned to a half-power (P/2) of the machine.

Figure 20a shows the starting time during 0.5 s, thereafter the operation is in permanent mode. The enlarging effect of the operation in permanent mode showing the voltage between phases of inverter A1 and stator current is shown in Figure 20b; the voltage between phases of inverter A2 and stator current is shown in Figure 20c. These results present the reduction in voltage source, which is half DC-link to give half-power of each inverter. Also, the quality of stator current is improved compared with classic induction machine.

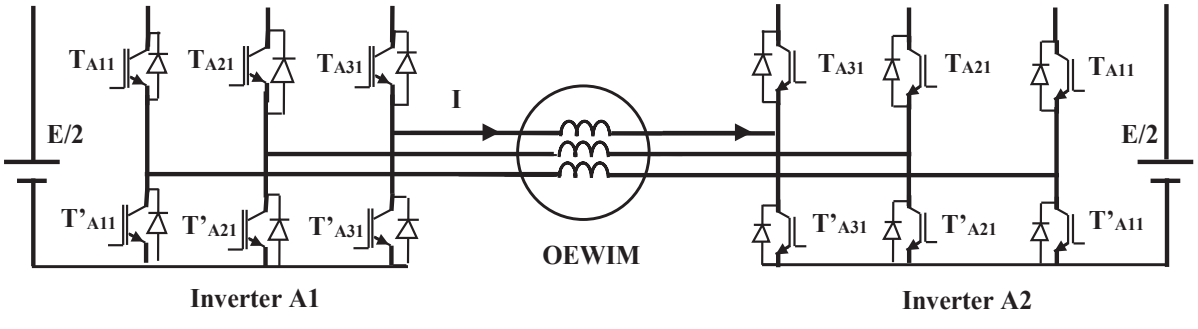

Figure 19. Open-end stator winding IM supplied by voltage source inverters.

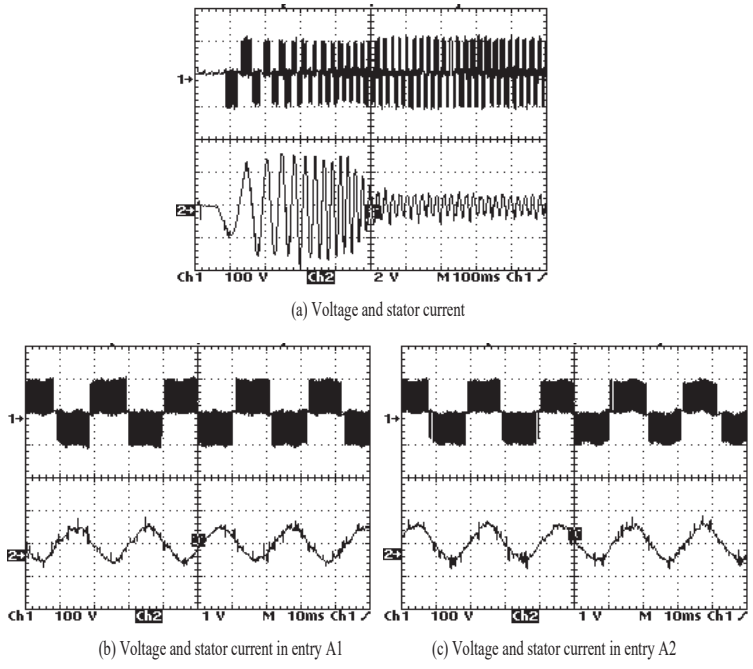

(a) Voltage and stator current

(b) Voltage and stator current in entry A1

(c) Voltage and stator current in entry A2

Figure 20. Experimental results of the open-end stator winding IM.

3.4. Experimental results for dual open-end stator windings induction machine

The feeding of the dual open-end stator winding asynchronous machine 'DOEWIM' fed by voltage source inverter with half DC-link to each input based on V/f law as represented in Figure 21. Each inverter is dimensioned to a quarter power of the machine.

Figure 22 shows the scalar control of the 'DOEWIM' with two stator currents in windings A and B. Thereafter the voltage between phases of machine and stator current in entry A1 is as presented in Figure 23.

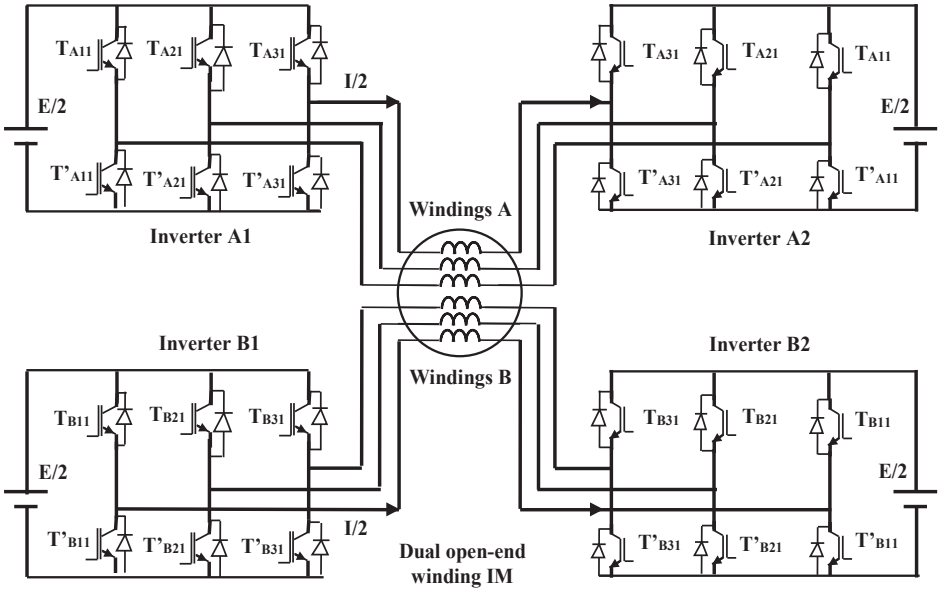

Figure 21. Supply of the 'DOEWIM' by voltage source inverters.

The obtained experimental results of the operation in permanent mode are shown by the voltages between phases of the entries A1 and A2 in Figure 24a; the same results as the entries B1 and B2 are shown in Figure 24b. The voltage between phases and stator current of the entry A1 is shown in Figure 24c; the same results of entry A2 are shown in Figure 24d. These results present the advantage compared with the classic induction machine at the level of the current and source voltage inverter, which is half-current and half DC-link to give a quarter power of each inverter.

Thereafter, this machine structure improves the quality of the stator current.

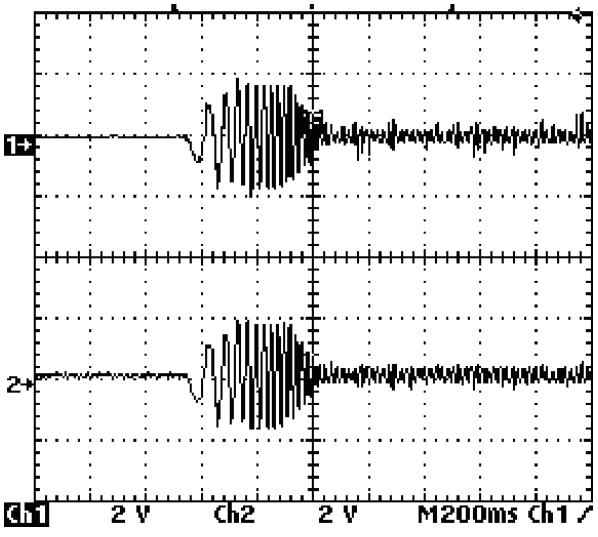

Figure 22. Stator current of windings A and B.

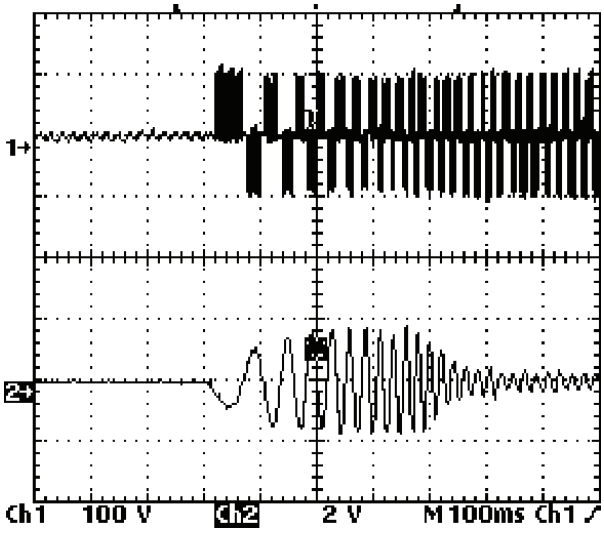

Figure 23. Voltage and stator current in entry A1.

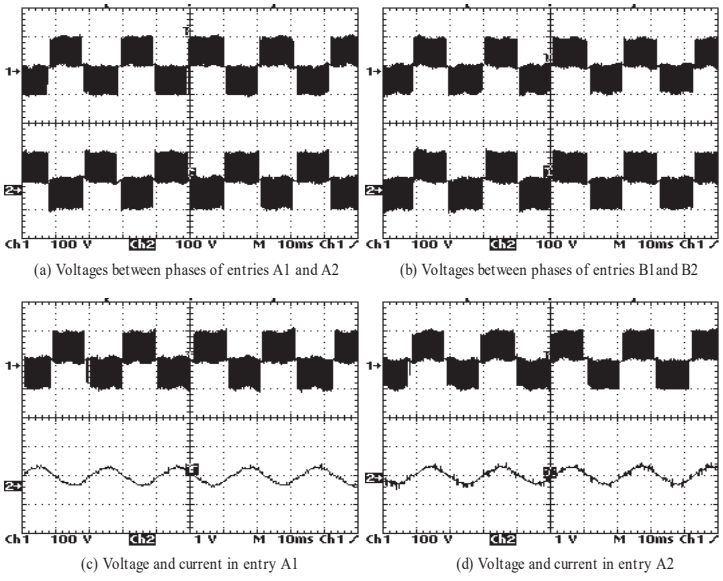

(a) Voltages between phases of entries A1 and A2 (b) Voltages between phases of entries B1and B2

(c) Voltage and current in entry A1 (d) Voltage and current in entry A2

Figure 24. Experimental results of the operation mode of the 'DOEWIM'.

4. Interpretation of Different Results

To view the performance of the induction machine with different stator winding structures, we used a single prototype of an induction machine to carry out the four machine structures controlled with scalar control of the same frequency and same dead-time. Experimental results show the importance of open-end stator winding induction machines; indeed, these machines compared with induction machines with one or two three-phase windings in star allow better power segmentation and offer more liberty degrees in a degraded mode. In addition, they offer a better quality of the stator current. Figure 25 shows the stator currents for the four machines and we can see the improvement in the quality of the stator current, especially for the dual open-end stator windings machine. Moreover, the open-end winding machine compared with the double star machine presents a better quality of stator current.

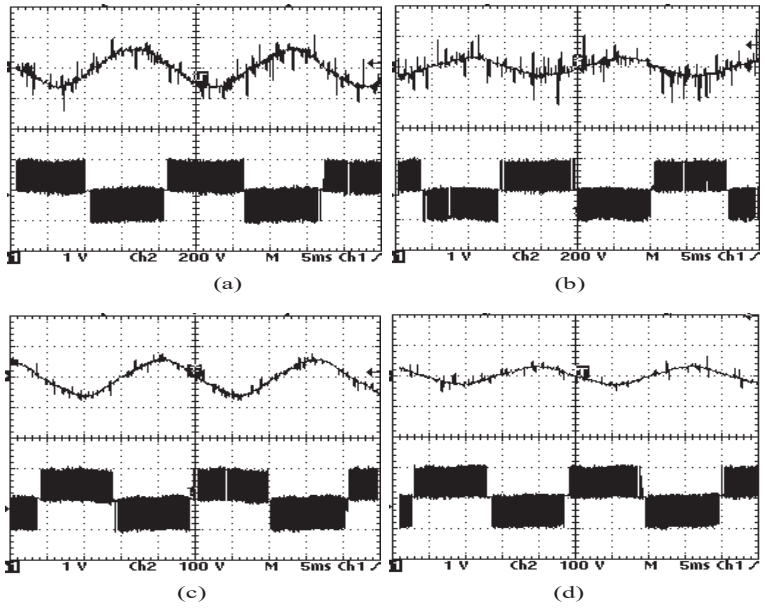

(a) (b)

(c) (d)

Figure 25. Experimental results of the stator current and voltage for the four machines: (a) classic IM, (b) double star IM, (c) open-end winding IM and (d) dual open-end winding IM.

5. Conclusion

The prototype of an induction machine with a nominal power P = 1.5 kW is designed to carry four machine structures which are the classical induction machine, the double star induction machine, the open-end stator winding induction machine and the dual three-phase open-end stator windings induction machine. Thereafter, these machines have been controlled by a scalar control with the same frequency and dead-time, for which the scalar is implemented on an FPGA board. The experimental results of the prototype of induction machine have shown significant advantages of the open-end winding machine structures. Indeed, the supply voltage for the 'OEWIM' is reduced by half compared with the conventional machine with the best quality of stator current. In addition, it offers one degree of freedom in degraded mode. Furthermore, the supply voltage for the 'DOEWIM' is also divided in half compared with the 'DSIM' with the best quality of stator current and offers three liberty degrees in degraded mode.

These obtained experimental results allow to conclude the interest of open-end windings induction machines at the level of power segmentation or operating in degraded mode, in particular the 'DOEWIM', which responds to the concept of Power Electronic Building Bloc (PEBB) initiated by the Office of Research Noval (ONR) and US Center of Power Electronics System (CPES), and aims to improve reliability, modularity, standardisation, scalability, re-configurability and reducing the cost of electrical systems.

References

Abbas, M. A., Christen, R. and Jahns, T. M. (1984). Six-Phase Voltage Source Inverter Driven Induction Motor. *IEEE Transactions on Industry Applications*, IA-20(5), pp. 1251–1259. doi: 10.1109/TIA.1984.4504591

Alger, P. L. (1928). The Calculation of the Armature Reactance of Synchronous Machines. *Transactions of the American Institute of Electrical Engineers*, 47, pp. 493–512.

Bodo, N., Levi, E. and Jones, M. (2013). Investigation of Carrier-Based PWM Techniques for a Five-Phase Open-End Winding Drive Topology. *IEEE Transactions on Industrial Electronics*, 60, pp. 2054–2065. doi: 10.1109/TIE.2012.2196013

Chatterjee, S. and Kastha, D. (2024). A New Multilevel Converter Configuration for Medium-Voltage Open-Winding PMSG-Based Wind Energy Conversion Systems. *IEEE Journal of Emerging and Selected Topics in Industrial Electronics*, 5(1), pp. 39–49. doi: 10.1109/JESTIE.2023.3293428

Guizani, S. and Ben Ammar, F. (2008). The Improvement Availability of a Double Star Asynchronous Machine Supplied by Redundant Voltage Source Inverter. *Journal of Electrical System JES*, 4,

Guizani, S. and Ben Ammar, F. (2013). The Dual Open-End Winding Induction Machine Fed by Quad Inverters in Degraded Mode. *International Journal of Scientific Engineering and Research*, 4, pp. 640–646.

Guizani, S. and Ben Ammar, F. (2015). Dual Open-End Stator Winding Induction Machine Fed by Redundant Voltage Source Inverters. *Turkish Journal of Electrical Engineering and Computer Sciences*, 23, pp. 2171–2181. doi: 10.3906/elk-1305-80

Guizani, S. and Ben Ammar, F. (2018). Torque and Current Enhancement Based on Dual Open-End Stator Winding IM at 0° Fed by Two 2-Level Cascaded Inverters. *Electrical Engineering*, 3, pp. 1869–1879. doi: 10.1007/s00202-017-0668-2

Jacek, L. (2018). Application of Super-Twisting Sliding Mode Controllers in Direct Field-Oriented Control System of Six-Phase Induction Motor: Experimental Studies. *Power Electronics and Drives*, 3(8), pp. 23–34. doi: 10.2478/pead-2018-0013

Jahns, T. M. (1980). Improved Reliability in Solid-State AC Drives by Means of Multiple Independent Phase-Drive Units. *IEEE Transactions on Industry Applications*, IA-16(3), pp. 321–331. doi: 10.1109/TIA.1980.4503793

Jiang, C., Liu, H., Wheeler, P., Wu, F. and Huo, J. (2023). An Optimized Modulation for Five-Phase Open-End Winding PMSM with Sliding Clamped Strategy. *IEEE Transactions on Industrial Electronics*, 70(9), pp. 8819–8829. doi: 10.1109/TIE.2022.3212385

Kalaiselvi, J. and Srinivas, S. (2015). Bearing Currents and Shaft Voltage Reduction in Dual-Inverter-Fed Open-End Winding Induction Motor with Reduced CMV PWM Methods. *IEEE Transactions on Industrial Electronics*, 62(1), pp. 144–152. doi: 10.1109/TIE.2014.2336614

Levi, E., Satiawan, I. N. W., Bodo, N. and Jones, M. (2012). A Space-Vector Modulation Scheme for Multilevel Open-End Winding Five-Phase Drives.

IEEE Transactions on Energy Conversion, 27(1), pp. 1–10. doi: 10.1109/TEC.2011.2178074

Monteiro, A. P., Jacobina, C. B., Bahia, F.A.d.C and De Sousa, R. P. R. (2022). Vienna Rectifiers for WECS Applications with Open-End Winding PMSM. *IEEE Transactions on Industry Applications*, 58(2), pp. 2268–2279. doi: 10.1109/TIA.2022.3142658

Nayli, A., Guizani, S. and Ben Ammar, F. (2017). Modeling and Analysis of the Novel Dual Open-End Stator Windings Wound Rotor Synchronous Machine with Dampers. *Turkish Journal of Electrical Engineering and Computer Sciences*, 25, pp. 995–1009. doi: 10.3906/elk-1506-250

Nelson, R. H. and Krause, P. C. (1974). Induction Machine Analysis for Arbitrary Displacement Between Multiple Winding Sets. *IEEE Transactions on Power Apparatus and Systems*, PAS-93(3), pp. 841–848. doi: 10.1109/TPAS.1974.293983

Sandulescu, A. P., Meinguet, F., Kestelyn, X., Semail, E. and Bruyere, A. (2013). Flux-Weakening Operation of Open-End Winding Drive Integrating a Cost-Effective High-Power Charger. *IET Electrical Systems in Transportation*, 3(1), pp. 10–21. doi: 10.1049/iet-est.2012.0026

Singh, G. K., Pant, V. and Singh, Y. P. (2003). Voltage Source Inverter Driven Multi-Phase Induction Machine. *Computers and Electrical Engineering*, 29, pp. 813–834. doi: 10.1016/S0045-7906(03)00036-3

Somasekhar, V. T., Baiju, M. R. and Gopakumar, K. (2004). Dual Two-Level Inverter Scheme for an Open-End Winding Induction Motor Drive with a Single DC Power Supply and Improved DC Bus Utilisation. *IEE Proceedings - Electric Power Applications*, 151(2), pp. 230–238. doi: 10.1049/ip-epa:20040023

Xueqing, W., Zheng, W., Wei, W. and Ming, C. (2018). Fault Diagnosis of Sensors for T-Type Three-Level Inverter-Fed Dual Three-Phase Permanent Magnet Synchronous Motor Drives. *Power Electronics and Drives*, 4(39), pp. 165–175.

Yu, Z., Chen, Y., Zhao, J., Zhang, X. and Zhou, X. (2025). Alternate Subhexagonal Center Dual-Inverter PWM Scheme for Open-End Winding DC-Biased-VRM Drive Using Adjustable Zero Voltage Vector with Dead-Time Effect Compensation. *IEEE Transactions on Transportation Electrification*, 11(3), pp. 7322–7333. doi: 10.1109/TTE.2025.3526609

Zerdani, M., Ardjoun, S. A. E. M., Chafouk, H. and Denai, M. (2023). Experimental Investigation of Decoupled Discontinuous PWM Strategies in Open-End Winding Induction Motor Supplied by a Common DC-Link. *IEEE Journal of Emerging and Selected Topics in Power Electronics*, 11(3), pp. 3087–3096. doi: 10.1109/JESTPE.2023.3258799